SECTION 2

THERMAL AND FAST REACTOR MATERIALS

UDK 669.017:539.16

HARDENING OF Cr-Fe-Ni-Mn HIGH-ENTROPY ALLOYS CAUSED BY THE IRRADIATION WITH ARGON IONS

G.D. Tolstolutskaya, G.Y. Rostova, V.N. Voyevodin, A.N. Velikodnyi, M.A. Tikhonovsky, G.N. Tolmachova, A.S. Kalchenko, R.L. Vasilenko, I.E. Kopanets
National Science Center "Kharkov Institute of Physics and Technology", Kharkov, Ukraine

Nanoindentation was used to measure the ion irradiation effect on hardening of Cr-Fe-Ni-Mn high-entropy alloys with different composition. Alloys were irradiated with 1.4 MeV Ar ions at room temperatures and midrange doses from 0.3 to 5 displacements per atom (dpa). Different methods of nanoindentation data processing were used to determine true values of nanohardness and calculate Vickers hardness and yield strength. It was shown that hardness and yield strength increase with irradiation dose, but this increasing lower than in stainless steel.

INTRODUCTION

Structural materials used in nuclear reactors must maintain both mechanical performance (strength, ductility, and fracture toughness) and dimensional stability (against creep and void swelling) under irradiation environments of various energetic particles [1]. To develop the next-generation nuclear reactor that will be more efficient and economical and produce less radioactive waste, the high-performance structural materials will be required to withstand severer environment, such as higher temperatures and irradiation doses, which exceeds the limits of current nuclear materials.

Within the past several years, a fundamentally new class of metallic alloys has been developed – high entropy alloys (so called HEAs) [2]. HEAs are defined as alloys consisting of 5 or more principal elements with nearly equiatomic fractions in range 5…35 at.%. Unlike traditional alloy designs, in which one major element is selected as the solvent and several dilute solute elements are added, all elements in HEAs are major.

Several compositions of HEAs or multicomponent alloys have been found to form ductile solid solution structures involving face centered cubic (FCC) or body centered cubic (BCC) phases or mixtures of the two, instead of brittle intermetallic compounds [2]. In addition, their attractive physical and mechanical properties such as high strength, ductility, wear resistance, high temperature softening resistance and corrosion resistance make HEAs potential candidates for high temperature fission or fusion structural applications. Their extraordinary mechanical properties have led to intensive interest in investigating their potential for practical applications, including nuclear power [3].

Knowledge of their irradiation response is, however, very limited, since the development of these alloys is fairly recent. Nonetheless, there is practically nothing known about their radiation resistance at elevated temperatures relevant for potential nuclear energy applications. It is hypothesized that the high configurational entropy might influence point defect recombination phenomena in irradiated materials by modifying the vacancy-interstitial recombination interaction distance, solute diffusivity, or other mechanisms, thereby producing different (superior or inferior) radiation stability compared to conventional single phase alloys. Radiation-induced hardening is a very important effect which must be taken into account, because when material is hardening it becomes brittle.

In order to obtain more mechanical property data, experiments in real reactor neutron irradiation environment should be carried out in a variety of operation conditions. However, they are usually costly and time consuming. The use of ion irradiation for the simulation of radiation damage produced by neutrons within reactors is now a common practice [4, 5], due to accelerated damage rates and absence of induced activation. However unlike neutrons, the electronic stopping limits the range of ion into a solid, typical low energy proton beam or MeV self-ions damaged layers have a thickness of the order of one micrometer below the irradiated sample surface. Therefore, nanoscale methods of testing irradiated materials with small volume need to be applied.

Many of the high entropy alloys with FCC crystal lattice studied to date contain cobalt, making them unfavorable for nuclear applications due to high neutron transmutation-induced radioactivity that can increase radiation shielding requirements during handling after neutron irradiation and can lead to undesirable increase in radiation exposures to workers during maintenance of nuclear power plants. For this reason high entropy alloy 18Cr-28Fe-27Mn-28Ni without Co has been developed [3]. We have developed two other high entropy alloys of Cr-Fe-Ni-Mn system: 18Cr-40Fe-28Mn-14Ni and 20Cr-40Fe-20Mn-20 Ni.

The aim of this study is to investigate these alloys for stability in relation to the development under the training of the hardening phenomenon and to establish the dependence of the hardening parameters on the irradiation dose and the structure of the alloys.

1. EXPERIMENTAL

Alloys with the compositions (in at.%) of 18Cr-40Fe-28Mn-14Ni (E30-2), 18Cr-28Fe-27Mn-28Ni (E31-2), and 20Cr-40Fe-20Mn-20Ni (E32-2) were

produced by arc melting in a high-purity argon in a water-cooled copper mould. The purities of the alloying elements were above 99.9%. To ensure chemical homogeneity, the ingots were flipped over and remelted a least 5 times. The produced ingots had dimensions of about 6×15×60 mm. The alloys were studied both in as-solidified state and after homogenization annealing. Homogenization was carried out at 1050 °C and lasted for 24 hours. Prior to homogenization samples were sealed in vacuumed (10^{-2} Torr) quartz tubes filled with titanium chips to prevent oxidation.

Alloys were subjected to thermomechanical treatment (TMT), that consisted in deformation of the rolling at room temperature from 6 to 0.2 mm with intermediate annealing at 1100 °C for 3 hours on the thicknesses of 2 and 0.8 mm. Finishing annealing on the thicknesses of 0.2 mm was carried out at two temperatures – 850 and 1050 °C for 1 hour. The structure of the alloys was studied by X-ray diffractometry (Dron-4, Cu Kα-radiation), metallography and electron microscopy JEM-100CX and JEM-2100.

Samples were irradiated with 1.4 MeV argon ions in a range of doses 0.3…5 dpa. All irradiations were carried out with accelerating-measuring system "ESU-2" [6], which contain Van de Graaf accelerator. The irradiation was performed at room temperature. The depth distribution of Ar atoms concentration and damage was calculated by SRIM 2008 [7] and shown in Fig. 1. The damage calculations are based on the Kinchin-Pease damage energy model, with a displacement energy of 40 eV for Fe and Cr, as recommended in ASTM E521-96 (2009) [8].

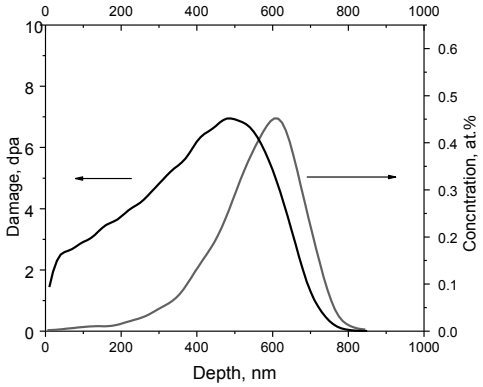

Fig. 1. Calculated profiles of damages and concentrations of 1.4 MeV Ar ions implanted to the dose of $1 \cdot 10^{17}$ cm^{-2}

Nanohardness was measured by Nanoindenter G200 with a Berkovich type indentation tip. Tests were performed with a constant deformation rate of 0.05 s^{-1}. Each sample was applied at least 10 prints at a distance of 35 μm from each other. The methodology of Oliver and Pharr was used to find the hardness [9]. The details of nanoindentation tests have been presented elsewhere [10].

In order to establish bulk equivalent hardness H_0 (or the hardness at infinite depth) from nanoindentation measurements we used three methods that mentioned in literature. The first and the most widely used method is based on combination of Nix – Gao model and a composite hardness model for the softer substrate effect – i. e. Kasada's model [11]. The next one method is proposed in [12]. Here the bulk equivalent hardness is calculated by an equation $H_{0,irr} = \sqrt{H_{test,irr}^2 - H_{test,unirr}^2 + H_{0,unirr}^2}$. And the last one method offered in [13] and based on the ratio of H_{irr}/H_{unirr} (where H_{irr} and H_{unirr} – is average nanohardness of irradiated and unirradiated samples, respectively) to characterize the increasing degree of hardness after irradiation.

2. RESULTS AND DISCUSSIONS

Alloys structure. According to X-ray analysis all as-cast alloys are single-phase and have FCC crystal lattice. After TMT and final heat treatment at 850 °C, the E31-2 alloy and E32-2 alloy are single-phase also, but the E30-2 alloy turned out to be biphase – in addition to the main FCC phase, there is a σ-phase in it.

Fig. 2 compares the microstructures of 18Cr-40Fe-28Mn-14Ni (E30-2), 18Cr-28Fe-27Mn-28Ni (E 31-2), and 20Cr-40Fe-20Mn-20Ni (E32-2) high entropy alloys final heat treatment at 850 °C before irradiation test.

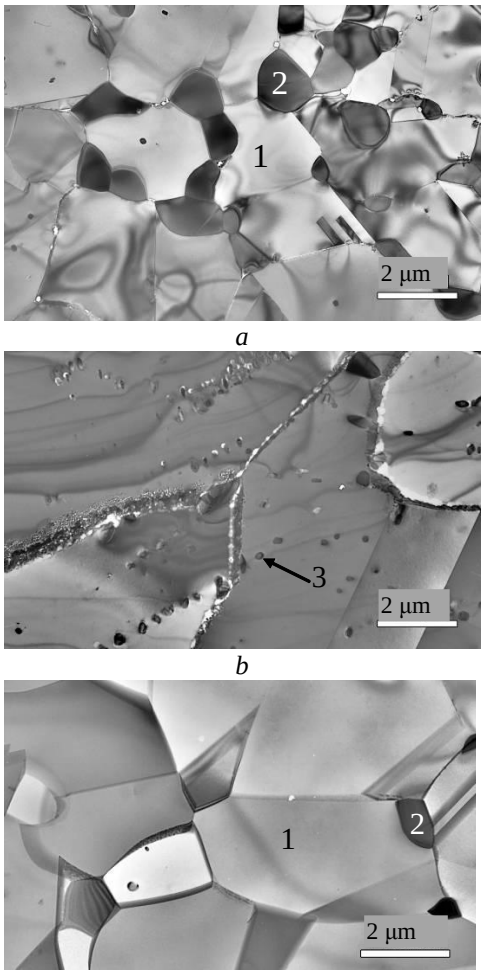

Fig. 2. The initial microstructure of 18Cr-40Fe-28Mn-14Ni (E30-2) (a), 18Cr-28Fe-27Mn-28Ni (E31-2) (b), and 20Cr-40Fe-20Mn-20Ni (E32-2) (c) alloys after heat treatment at 850 °C (1 – FCC phase; 2 – σ-phase; 3 – complex oxides)

The bright field images combining with the corresponding selected area electron diffraction patterns, also show that the E30-2 alloy consist of FCC phase+ σ-phase (see Fig. 2,a). E31-2 and E32-2 alloys are nearly single-phase (see Fig. 2,b,c). Small inclusions in E31-2 alloy (see Fig. 2,b) are complex (Cr, Mn) oxides and negligible amount of σ-phase is detected in E32-2 samples (see Fig. 2,c).

After final annealing at 1050 °C all samples contain only FCC phase.

Nanohardness. Fig. 3 shows indentation-depth profiles of nanohardness of 18Cr-40Fe-28Mn-14Ni (E30-2), 18Cr-28Fe-27Mn-28Ni (E31-2), and 20Cr-40Fe-20Mn-20Ni (E32-2) high entropy alloys before and after ion irradiation with argon ions to damage doses 0.3…5 dpa.

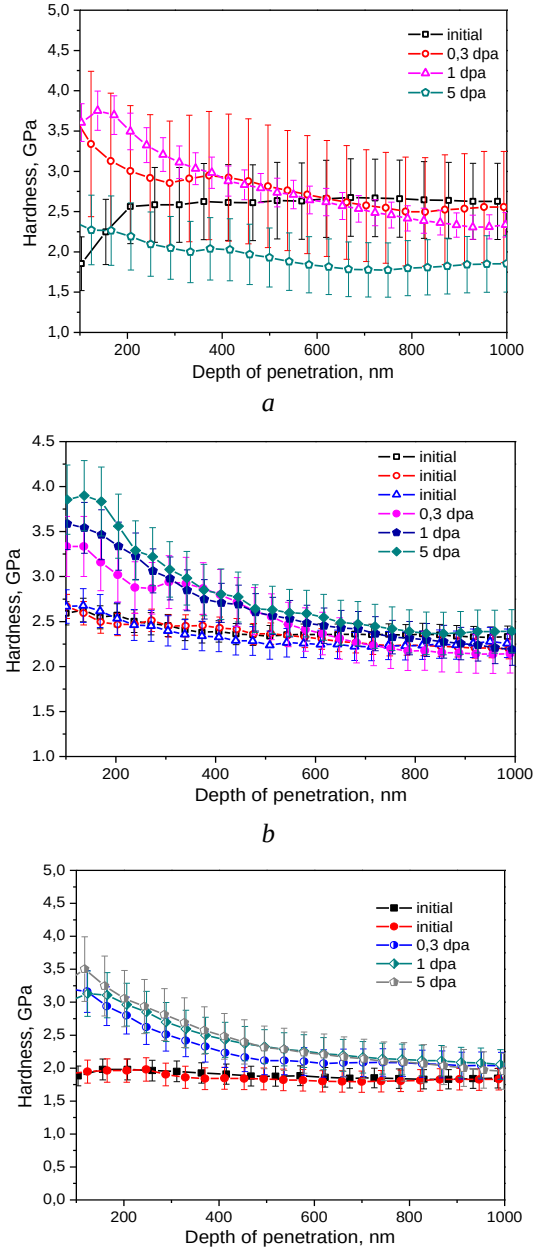

Fig. 3. The profiles of nanoindentation hardness in the direction of depth for E30-2 (a), E31-2 (b), and E32-2 (c) alloys before and after 1400 keV/Ar^+ beam irradiation (temperature of the final heat treatment of specimens is 850 °C)

This interval of doses was chosen because G.S. Was et al. analyzing the data of radiation induced segregation, irradiated microstructure, radiation hardening and IASCC susceptibility of the same heats of proton- and neutron-irradiated 304SS and 316SS have shown that the irradiation hardening of austenitic steels saturates at doses about a few dpa [14]. The correlation between radiation-induced hardening and microstructure evolution in SS316 stainless steal irradiated with 1.4 MeV Ar^+ ions in the dose range of 0…25 dpa at 300 and 900 K has been studied. It is established that the hardening at specified damaging doses reaches 75% and tends to saturation at 2 dpa [15].

Fig. 4 summarizes the measured hardness of the pristine and irradiated regions of the three alloys. As it can be seen, there is essential scatter in nanoindentation data, especially for E30-2 alloy. The minimum scatter is observed for E32-2 sample. To our mind, this occurs due to microstructural heterogeneity of alloys, e.g. presence of sigma phase an oxide phase (see Fig. 2). However, as a trend, we can state that in the initial samples the hardness is 2…2.5 GPa, while in irradiated ones it grows to 3.5 GPa.

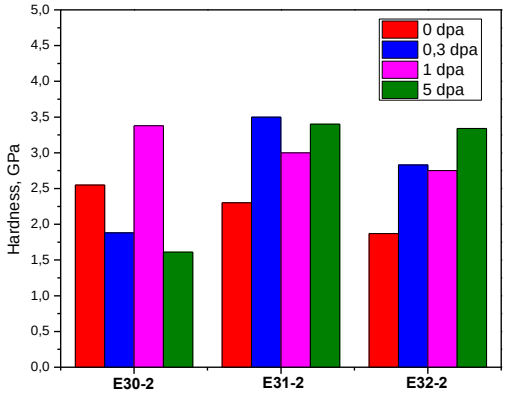

Fig. 4. Nanohardness before and after irradiation for E30-2, E31-2, and E32-2 alloys

That's why next experiments were carry out on the samples from E32-2 alloy which were heat treated at 1050 °C and not contain any inclusions of second phase.

Fig. 5,a,b shows graphs H (h) and H^2(1/h) for these samples in initial state and after ion irradiation in a range of doses 0.3…5 dpa. It can be seen that the scatter of dates is much smaller than in samples which were heat treated at 850 °C (see Fig. 3). H_0 is estimated from curve averaged over 10 indents (see Fig. 5,c). The procedure of the estimation is described below.

Standard methods of evaluation of hardness measured by nanoindentation tests do not allow to take into account many effects that affect the true nanohardness value (such as indentation size effect, the presence of sink in/pile up, degree of surface roughness and other artifacts). In particular, Oliver and Pharr method [9], which allows to set the values of nanohardness from the "load – depth of penetration" curves does not take into account the influence of the indentation size effect (ISE), when the hardness increase with reducing the load on the indenter tip. Nix – Gao model is used to account the influence of the size effect on true values of nanohardness, based on the concept of

geometrically necessary dislocations that occur under the indenter tip during measuring of hardness [16].

There are a few papers, in which radiation hardening is evaluated using the Nix and Gao model. In particular, Kasada et al. have suggested a new model to extrapolate the experimentally obtained nanoindentation hardness to the bulk-equivalent hardness of ion-irradiated Fe-based binary model alloys [11]. This model is based on a combination of the Nix – Gao model for the indentation size effect and a composite hardness model for the softer substrate effect (SSE) of the nonirradiated region beyond the irradiation range. The hardness of bulk sample H_0 can be obtained if plot the graph H^2 (1/h). The square root of the value obtained by the intersection of the tangent to curve $H^2 = f$ (1/h) with the H^2 axis gives the value of H_0.

The way how to estimate bulk equivalent hardness (hardness of bulk material) we discussed in details in [17].

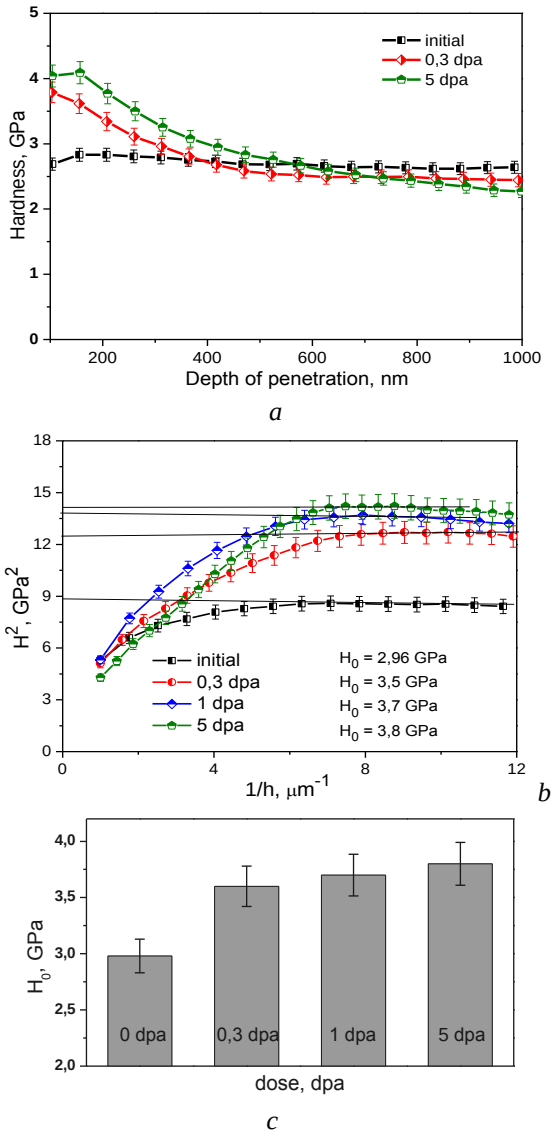

Fig. 5. Indentation depth dependence of hardness (a), curves of H^2–1/h for nanoindentation hardness (b) and diagram of hardening (c) for initial and irradiated E32-2 alloy (temperature of the final heat treatment of specimens is 1050 °C)

Fig. 5,a gives the average nanoindentation hardness of all indents with error bars in high entropy alloy E32-2 in order to highlight the depth dependence of hardness. It is clearly seen that there is a hardness increase after irradiation especially in the near surface region (less than 600 nm).

The hardness data was plotted as H^2 versus 1/h to compare with the Nix – Gao model in Fig. 5,b. Unirradiated samples have a good linearity above 100 nm. However, the irradiated samples appear to have a bilinearity in the range of > 100 nm. It is also shown that plots of irradiated alloys have an inflection at ~ 143 nm. Under the critical indentation depth, unirradiated softer substrate can contribute to the hardness with increasing the indent depth. Ignoring the shallow radiation damage and stopping peak region effects, here we use Kasada method to calculate H^{irr}_0 in the range of 100 nm < h < 150 nm.

The highest hardness shows irradiated to 5 dpa sample – 3.8 GPa, than 1 dpa – 3.7 GPa, and 0.3 dpa – 3.6 GPa. Hardness of the unirradiated sample is 2.96 GPa. As can be seen, the hardening of irradiated samples is less than two times in comparison with unirradiated one and the difference in hardness values of irradiated samples is insignificant. The highest hardness increasing demonstrates sample irradiated to 5 dpa (≈ 1.28 times, ≈ 28%), than – 1 dpa (≈ 25%), and 0.3 dpa (≈ 22).

It should be noted that Nix – Gao model is based on the assumption that an indentation results in the generation of geometrically necessary dislocations (GNDs) within the semi-sphere under the indent. However, Katoh, et al. observed by TEM the cross-section of indented region [18] and revealed that in ferrous alloys the GND affected zone strongly depended on the indentation depth: the GND zone was anisotropic when the indentation depth is less than 100 nm, but it was quite semispherical when exceeding 300 nm. This fact indicates that Nix – Gao model does not fit at a shallow area but fits well in deep area. As a result, the bulk-equivalent hardness of the unirradiated specimen could still be estimated by Nix – Gao plots of the deeper area. The hardness of the irradiated layer in the shallow area needs a more adequate evaluation method.

There are at least two analytical methods to estimate radiation-induced hardening measured by nano-indentation method:

1) The hardness of unirradiated material, $H_{test,unirr}$, is directly subtracted from the hardness of irradiated material, $H_{test,irr}$ (see Eq. (1)), based on the assumption that the size effect is the same for the hardness before and after irradiation [19]. Both hardness values ($H_{test,unirr}$ and $H_{test,irr}$) are measured by nanoindentation test.

$$\Delta H = H_{test,irr} - H_{test,unirr}. \qquad (1)$$

2) An application of Nix-Gao model which provides the bulk-equivalent hardness H_0, based on GND concept.

Zhang et al. [12] combined these two methods and received an equation system (2).

$$\begin{aligned} H^2_{test,irr} - H^2_{0,irr} &= \left(kM\alpha\mu b\right)^2 \rho_{G,irr}, \\ H^2_{test,unirr} - H^2_{0,unirr} &= \left(kM\alpha\mu b\right)^2 \rho_{G,unirr}, \end{aligned} \qquad (2)$$

where $H_{test,irr}$ and $H_{test,unirr}$ – are measured values obtained by nanoindentation tests; k – is the coefficient between hardness and tensile stress; M – stands for Taylor's factor; α – is the hardening factor, μ – is the shear modulus; b – is the burgers vector; $\rho_{G,irr}$ and $\rho_{G,unirr}$ are the density of GND of irradiated and unirradiated samples, respectively.

The authors propose an analytical method of evaluating the hardness without taking into account the size effect, but only assuming that the density of geometrically necessary dislocations ρ_G before and after irradiation are identical, and the value of ρ_G depends only on the depth of indentation. Considering all the assumptions they obtained the Eq. (3).

$$H_{0,irr} = \sqrt{H^2_{test,irr} - H^2_{test,unirr} + H^2_{0,unirr}} \quad , \qquad (3)$$

where $H_{test,irr}$ and $H_{test,unirr}$ are measured values obtained by nanoindentation tests. $H_{0,unirr}$ is the bulk-equivalent hardness of unirradiated material, which could be estimated by the Nix – Gao model for deep depth.

Eq. (3) makes it possible to calculate the hardness of the irradiated layer without discussion of the real distribution and densities of geometrically necessary dislocations.

Figs. 6 and 7 demonstrate diagrams of H_0 values and hardening obtained from Eq. 3 for unirradiated and irradiated samples.

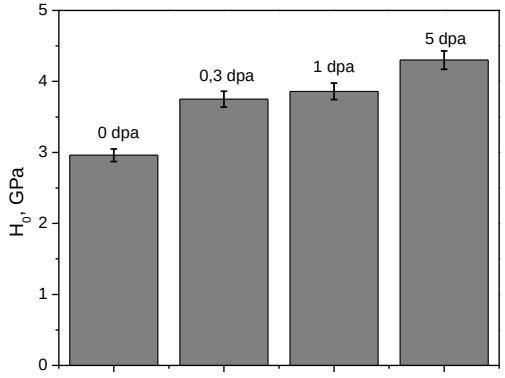

Fig. 6. The estimated bulk equivalent hardness of E32-2 alloy after irradiation to 0.3…5 dpa, obtained from Eq. 3

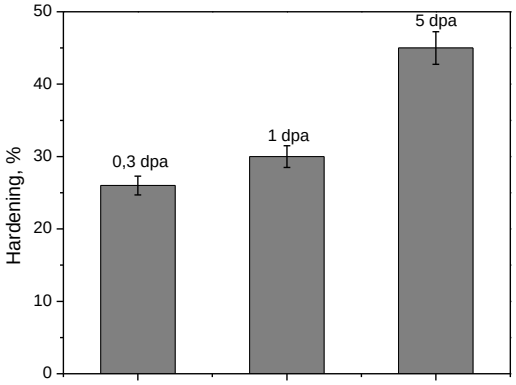

Fig. 7. Radiation-induced relative hardening of E32-2 alloy

Apparently, the hardness and the hardening of irradiated E32-2 alloy increases with dose increasing. The highest value of hardness has a sample irradiated to the highest dose (5 dpa) – 4.3 GPa. The hardening of irradiated sample comprised 26% for 0.3 dpa, 30% for 1 dpa, and 45% for 5 dpa. Values of hardness obtained from Eq. 3 are quite higher than that received from Kasada's model. Likely, this is due to adjustments that are not taken into account in Kasada's model.

Thus, the maximum hardening, which is obtained for high entropy alloys, taking into account different treatments of the experimental data, is about 30…40%. Consequently, these alloys lose less plasticity in comparison with traditional materials of nuclear power – austenitic steels 18Cr10NiTi and SS316 – for which hardening after identical irradiation almost doubles [17].

Aidhy et al. [20] reported that the defect migration barriers and extended defect formation energies are higher in the multi-component disordered solid solution alloys than the pure metal, and their work hint that the defect concentration generated due to irradiation in FCC HEAs may be lower than that in traditional low-entropy alloys. Furthermore, many investigations have shown that atomic diffusion in multi-component disordered solid solution HEA is suppressed, resulting in much lower atomic mobility's. Tsai et al. [21] reported the sluggish diffusion in disordered CoCrFeMnNi HEA in comparison with pure metals and low-entropy alloys, and proposed that great fluctuation of lattice potential energy causes the significant atomic traps and blocks, leading to the high activation energies and low diffusion mobilities. Lower atomic mobilities in disordered solid solution HEAs than low-entropy alloys (including ordered compounds) may partly contribute to the greater resistance to irradiation than the latter.

To compare effect of hardening in different materials (as well as the same material irradiated by various doses) the ratio $H^{irr}_{av}/H^{unirr}_{av}$ is used to characterize hardness increasing after irradiation [13]. Fig. 8 shows dependence of the ratio of $H^{irr}_{av}/H^{unirr}_{av}$ on indentation depth in E32-2 alloy irradiated to 0.3, 1, and 5 dpa. Just about from a depth of 100 nm the hardness will decrease with the increase of indentation depth.

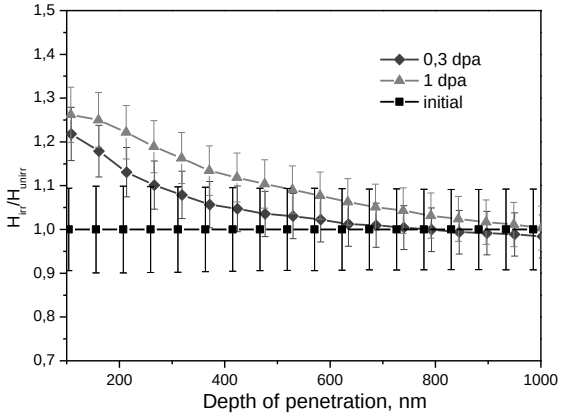

Fig. 8. Dependence of the ratio of H_{irr}/H_{unirr} on indentation depth in irradiated E32-2 alloy

Hosemann et al. [22] pointed out three effects should be considered in obtaining the value of hardness through hardness-depth curves. These effects are dose profile (damage grade) effects (DGE), indentation size effects (ISE), and implantation and surface effects.

Fig. 9 shows a schematic representation for this situation in hardening. For irradiated samples, the

implantation depth (I_d) is a key parameter [13]. If the radius of hemispherical influence zone is beyond it, the SSE will begin to take effect and the hardening ratio will decrease.

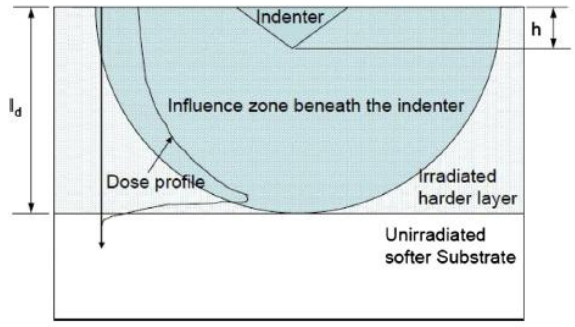

Fig. 9. Schematic representation for the transition of $H^{irr}_{av}/H^{unirr}_{av}$ ratio. The influence zone is assumed to be a hemispherical region beneath the indenter [13]

For 1.4 MeV Ar-ions the transition line stands at the depth about 140 nm which is about one fifth of the damaged layer thickness. This transition depth dependence behavior agrees approximately with the reports of hardening evaluation of single crystal copper, Fe-Cu(Mn) alloys and F82H steels irradiated by various ions [13].

It is rather difficult to extrapolate nanohardness to macroscopic properties such as Vickers hardness HV and yield strength σ_y based on these measurements. Works of Kang et al. and Takayama et al. [23, 24] showed that conventional Vickers hardness varied with nanoindentation hardness in a line way. Based on these data, a correlation equation is fitted.

$$H_0 = 0.01HV + 0.025\ , \quad (4)$$

$$\sigma_y = 3.03HV\ , \quad (5)$$

where H_0 is expressed in GPa, HV – in kg/mm^2 and σ_y is expressed in MPa [25]. Meanwhile the ΔHV was also converted to equivalent Δσ using a relation developed by Busby [25].

Fig. 10 shows dependence of calculated from Eq. 4 and 5 change of mechanical properties (Vickers hardness HV and yield strength σ_y) of E32-2 alloy from dose. Values of H_0 taken for this calculation are data that received from Kasada's model (see Fig. 5,c). As can be seen, change of Vickers hardness, and yield strength are increasing with dose rising.

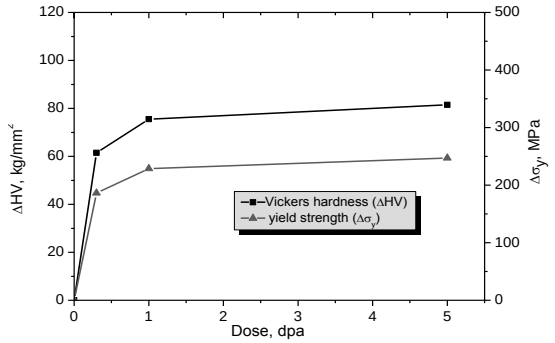

Fig. 10. Dependence of calculated change of Vickers hardness (ΔHV) and yield strength ($\Delta\sigma_y$) of E32-2 high entropy alloy from dose. H_0 received from Kasada's model

In addition, we defined change of Vickers hardness and yield strength from bulk-equivalent hardness values H_0, obtained by Eq. 3 (Fig. 11).

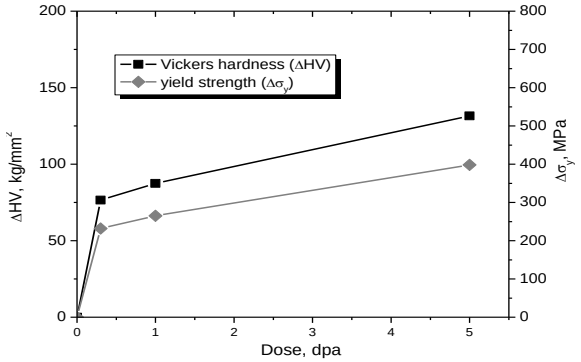

Fig. 11. Dependence of calculated change of Vickers hardness (ΔHV) and yield strength ($\Delta\sigma_y$) of E32-2 high entropy alloy from dose. H_0 received from Zhang's model

Evidently, values change of Vickers hardness and yield strength obtained from Eq.3 are higher than that received from Kasada's model. Trends of resulting curves are rather different (see Figs. 10, 11). Therefore, further detailed experimental investigations are required for more accurate assessments.

CONCLUSIONS

Nanoindentation was used to measure the ion irradiation effect on hardening of three Cr-Fe-Ni-Mn high-entropy alloys: 18Cr-40Fe-28Mn-14Ni (E30-2), 18Cr-28Fe-27Mn-28Ni (E31-2), and 20Cr-40Fe-20Mn-20Ni (E32-2). The final heat treatment of alloys before irradiation was carrying out at 850 and 1050 °C. Nanoindentation hardness of the samples which were heat treated at 850 °C show the tendency to increasing on irradiation dose, but scatter of dates is very high. The reason of such scatter is inclusions of second phase in alloys. The scatter of dates in samples of E32-2 alloy which were heat treated at 1050 °C was much smaller because second phases in it are absent.

We used different common methods of nanoindentation data processing to determine true values of nanohardness in these alloy. The main conclusions are as follows.

The highest value of hardness 4.3 GPa has the alloy irradiated to the highest dose (5 dpa), compared with hardness of the unirradiated sample is 2.96 GPa.

The hardening of irradiated E32-2 alloy increases with dose increasing and is 22…26% for 0.3 dpa, 25…30% for 1 dpa, and 28…45% for 5 dpa. The spread of data is determined by the methods of processing experimental data.

High-entropy alloys must lose less plasticity in comparison with traditional materials of nuclear power – austenitic steels X18H10T and SS316 – for which hardening after identical irradiation almost doubles.

REFERENCES

1. J.W. Yeh, Y.L. Chen, S.J. Lin, and S.K. Chen High-entropy alloys – a new era of exploitation // *Materials Science Forum*. 2007, v. 560, p. 1-9.

2. T. Nagase, P.D. Rack, J.H. Noh, T. Egami. In-situ TEM observation of structural changes in nano-crystalline CoCrCuFeNi multicomponent high-entropy alloy (HEA) under fast electron irradiation by high voltage electron microscopy (HVEM) // *Intermetallics.* 2015, v. 59, p. 32-42.

3. K. Jin; C. Lu, L.M. Wang, J. Qu, W.J. Weber, Y. Zhang, and H. Bei. Effects of compositional complexity on the ion-irradiation induced swelling and hardening in Ni-containing equiatomic alloys // *Scr. Mater.* 2016, v. 119, p. 65-70

4. G.D. Tolstolutskaya, V.V. Ruzhytskiy, S.A. Karpov, I.E. Kopanets. Features of retention and release of deuterium out of radiation-induced damages in steels // *Problems of atomic science and technology. Series "Physics of Radiation Damages and Effects in Solids".* 2009, N 4-2(62), p. 29-41.

5. В.Н. Воеводин, И.М. Неклюдов. *Эволюция структурно-фазового состояния и радиационная стойкость конструкционных материалов.* К.: «Наукова думка», 2006, 376 с.

6. G.D. Tolstolutskaya, V.V. Ruzhytskiy, I.E. Kopanetz, V.N. Voyevodin, A.V. Nikitin, S.A. Karpov, A.A. Makienko, T.M. Slusarenko. Accelerating complex for study of helium and hydrogen behavior in conditions of radiation defects generation // *Problems of atomic science and technology. Series "Physics of Radiation Damages and Effects in Solids".* 2010, N 1, p. 135-140.

7. http://www.srim.org/

8. ASTM E521-96, 2009, ASTM.

9. W.C. Oliver, G.M. Pharr. An improved technique for determining hardness and elastic modulus using load and displacement sensing indentation experiments // *J. Mater. Res.* 1992, v. 7, N 6, p. 1564-1583.

10. G.N. Tolmachova, G.D. Tolstolutskaya, S.A. Karpov, B.S. Sungurov, R.L. Vasilenko. Application of nanoindentation for investigation of radiation damage in SS316 stainless steel // *Problems of atomic science and technology. Series "Physics of Radiation Damages and Effects in Solids"*. 2015. N 5(99), с. 168-173.

11. R. Kasada et al. A new approach to evaluate irradiation hardening of ion-irradiated ferritic alloys by nano-indentation techniques // *Fusion Eng. Des*. 2011, v. 86, p. 2658-2661.

12. Z. Zhang, E. Hasenhuetl, K. Yabuuchi, A. Kimura. Evaluation of helium effect on ion-irradiation hardening in pure tungsten by nano-indentation method // *Nuclear Materials and Energy*. 2016, v. 9, p. 539-546.

13. Xiangbing Liu et al. Evaluation of radiation hardening in ion-irradiated Fe based alloys by nanoindentation // *J. Nucl. Mater.* 2014, v. 444, N (1-3). p. 1-6.

14. G.S. Was et al. Emulation of neutron irradiation effects with protons: validation of principle // J*ournal of Nuclear Materials.* 2002, v. 300, p. 198-216.

15. S.A. Karpov, G.D. Tolstolutskaya, B.S. Sungurov, A.Yu. Rostova, G.N. Tolmacheva, I.E. Kopanets. Hardening of SS316 Stainless Steel Caused by the Irradiation with Argon Ions // *Materials Science*. 2016, v. 52, issue 3, p. 377-384.

16. W.D. Nix, H.J. Gao. Indentation size effects in crystalline materials: A law for strain gradient plasticity // *J. Mech. Phys. Solid*. 1998, v. 46, p. 411-425.

17. G.D. Tolstolutskaya, S.A. Karpov, G.Y. Rostova, B.S. Sungurov, G.N. Tolmachova. The effect of irradiation with inert gas and hydrogen ions on nanohardness of SS316 stainless steel // *Вісник ХНУ, серія «Фізика».* 2015, в. 3, с. 66-70.

18. Y. Katoh, M. Ando, A. Kohyama. Radiation and helium effects on microstructures, nano-indentation properties and deformation behavior in ferrous alloys // *J. Nucl. Mater.* 2003, v. 323, p. 251-262.

19. P. Dayal, D. Bhattacharyya, W.M. Mook, et.al. Effect of double ion implantation and irradiation by Ar and He ions on nano-indentation hardness of metallic alloys *// J. Nucl. Mater*. 2013, v. 438, p. 108-115.

20. D.S. Aidhy, C.Y. Lu, K. Jin, H.B. Bei, Y.W. Zhang, L.M. Wang, W.J. Weber. // *Acta Mater*. 2015, v. 99, p. 69-76.

21. M.-H. Tsai, H. Yuan, G. Cheng, W. Xu, W.W. Jian, M.-H. Chuang, Ch.-Ch. Juan, S.-J. Lin, Y. Zhu. Significant hardening due to formation of a sigma phase matrix in a high entropy alloy // *Intermetallics.* 2013, v. 33, p. 81-86.

22. P. Hosemann, J.G. Swadener, D. Kiener, G.S. Was, S.A. Maloy, N. Li. An exploratory study to determine applicability of nano-hardness and micro-compression measurements for yield stress estimation // *Journal of Nuclear Materials.* 2008, v. 375, p. 135-143.

23. S.K. Kang, J.Y. Kim, C.P. Park, H.U. Kim, D. Kwon. Conventional Vickers and true instrumented indentation hardness determined by instrumented indentation tests // *J. Mater. Res*. 2010, v. 25, p. 337-343.

24. Y. Takayama, R. Kasada, Y. Sakamoto, et al. Nanoindentation hardness and its extrapolation to bulk-equivalent hardness of F82H steels after single- and dual-ion beam irradiation // *J. Nucl. Mate*r. 2013, v. 442, p. S23-S27.

25. J.T. Busby, M.C. Hash, G.S. Was. The relationship between hardness and yield stress in irradiated austenitic and ferritic steels // *J. Nucl. Mater.* 2005, v. 336, p. 267-278.

Article received 04.10.2017

РАДИАЦИОННОЕ УПРОЧНЕНИЕ ВЫСОКОЭНТРОПИЙНЫХ СПЛАВОВ Cr-Fe-Mn-Ni, ИНДУЦИРОВАННОЕ ОБЛУЧЕНИЕМ ИОНАМИ АРГОНА

Г.Д. Толстолуцкая, А.Ю. Ростова, В.Н. Воеводин, А.Н. Великодный, М.А. Тихоновский, Г.Н. Толмачева, А.С. Кальченко, Р.Л. Василенко, И.Е. Копанец

Наноиндентирование использовали для измерения эффекта ионного облучения на упрочнение высокоэнтропийных сплавов Cr-Fe-Ni-Mn различного состава. Сплавы облучали ионами 1,4 МэВ Ar^+ при комнатной температуре до доз от 0,3 до 5 смещений на атом (сна). Для определения истинных значений нанотвердости, а также для вычисления твердости по Виккерсу и предела текучести, использовались различные методы обработки данных наноиндентирования. Показано, что значения твердости и предела текучести растут с ростом дозы, но этот прирост меньше, чем в нержавеющих сталях.

РАДІАЦІЙНЕ ЗМІЦНЕННЯ ВИСОКОЕНТРОПІЙНИХ СПЛАВІВ Cr-Fe-Mn-Ni, ІНДУКОВАНЕ ОПРОМІНЕННЯМ ІОНАМИ АРГОНУ

Г.Д. Толстолуцька, Г.Ю. Ростова, В.М. Воєводін, О.М. Великодний, М.А. Тихоновський, Г.М. Толмачова, О.С. Кальченко, Р.Л. Василенко, І.Є. Копанець

Наноіндентування використовували для вимірювання ефекту іонного опромінення на зміцнення високоентропійних сплавів Cr-Fe-Ni-Mn різноманітного складу. Сплави опромінювали іонами 1,4 МеВ Ar^+ при кімнатній температурі до доз від 0,3 до 5 зміщень на атом (зна). Для визначення дійсних значень нанотвердості, а також для обчислення твердості за Віккерсом та межі плинності, використовувалися різні методи обробки даних наноіндентування. Показано, що значення твердості та межі плинності зростають із ростом дози, але цей приріст менший, ніж у нержавіючих сталях.